Momentum Dependence of Nuclear Mean Field and multifragmentation in Heavy-Ion Collisions

Yogesh K. Vermani, Supriya Goyal and Rajeev K. Puri *
Department of Physics, Panjab University,
Chandigarh-160014, India.

December 28, 2009

Abstract

We report the consequences of implementing momentum dependent interactions (MDI) on multifragmentation in heavy-ion reactions over entire collision geometry. The evolution of a single cold nucleus using static soft equation of state and soft momentum dependent equation of state demonstrates that inclusion of momentum dependence increases the emission of free nucleons. However, no heavier fragments are emitted artificially. The calculations performed within the framework of *quantum molecular dynamics* approach suggest that MDI strongly influence the system size dependence of fragment production. A comparison with ALADiN experimental data justifies the use of momentum dependent interactions in heavy-ion collisions.

1 Introduction

The heavy-ion collisions have always played a fascinating role in exploring various aspects of nuclear dynamics such as fission-fusion [1, 2, 3], multifragmentation [4, 5, 6, 7, 8, 9, 10, 11, 12], collective flow [6, 9, 13, 14, 15, 16, 17] as well as particle production [5, 18, 19] etc. The wider energy spectrum available due to modern accelerator technologies has become a powerful tool in experimental

*rkpuri@pu.ac.in

and theoretical studies in exploring the nature of hot and compressed nuclear medium via heavy-ion collisions.

It is well accepted that the outcome of a reaction depends not only on the density but also on the momentum space [18, 20]. The momentum dependence of the equation of state can be extracted from the real part of the optical potential. This potential is expected to affect those nucleons from target and projectile which possess larger relative momenta. The momentum dependence of the nucleon-nucleon (n-n) potential is found to affect drastically the collective flow observables [21, 22] and particle production [4, 18, 19]. It has been shown that observables related to the particle production *e.g.* π, κ, λ yields, n_d/n_p ratios etc. are strongly influenced by the momentum dependence of the n-n interaction [18, 19]. A strong influence of momentum dependent interactions was also observed on fragment flow for $E_{lab} \geq 400\ MeV/nucleon$. In higher incident energy regime, momentum dependent interactions (MDI) cause stronger reduction in the number of n-n collisions leading to more pronounced transverse flow. The momentum dependent interactions, therefore, increase the mean free path of nucleons, and consequently affect the stopping and thermalization of nuclear matter [21, 23].

On the contrary, very few attempts exist in the literature, that shed light on the consequences of implementing momentum dependent interactions in fragmentation [10, 22]. One of the basic problem with MDI is the strong repulsion created in the nuclear environment. As a result, nuclei propagating with MDI tend to be destabilized and start decaying via emission of free nucleons and clusters quite early during the reaction. Interestingly, the role of momentum dependent interactions depends crucially on the impact parameter of the reaction. It is found to enhance the energy of disappearance of flow in central collisions [15], whereas it reduces the energy of disappearance of flow in peripheral collisions [16, 17]. Similarly, MDI reduce the production of fragments in central collisions whereas it enhances the same in peripheral collisions [22]. However, one always remained concerned about the stability of nuclei propagating with momentum dependent interactions. Even a use of cooling procedure via Pauli potential is also reported in the literature [7]. Our present aim, therefore, is to investigate the stability of cold nuclei propagating under the influence of momentum dependent interactions and to see whether one can study fragmentation with MDI or not. An attempt to study the system size effects in the presence of momen-

tum dependent forces will also be made. We shall also confront our calculations with multifragmentation data of ALADiN group [11] which has a *rise and fall* variation with impact parameter. This study is carried within the framework of quantum molecular dynamics (QMD) transport model [4, 5]. The QMD model and implementation of momentum dependent potential are described in section 2. Our results are presented in section 3 and summarized in section 4

2 QMD Model and Momentum Dependent Interactions

The quantum molecular dynamics (QMD) model [4, 19] is an n-body transport theory that simulates the heavy-ion (HI) reactions between 30 MeV/nucleon and 1 GeV/nucleon on event by event basis. It includes quantum features like Pauli blocking, stochastic scattering and particle production. Here each nucleon is represented by Wigner distribution function of the form:

$$f_i(\mathbf{r},\mathbf{p},\mathbf{t}) = \frac{1}{(\pi\hbar)^3} e^{-(\mathbf{r}-\mathbf{r}_i(t))^2/2L} . e^{-(\mathbf{p}-\mathbf{p}_i(t))^2 2L/\hbar^2}, \tag{1}$$

where $\mathbf{r_i(t)}$ and $\mathbf{p_i(t)}$ define the classical orbit, the center of i^{th} Gaussian wave packet in phase space which evolves in time. The centers of these Gaussian wave packets propagate according to the classical equations of motion [4, 6]. The interaction part used in the QMD model consists of local Skyrme interaction, a finite range Yukawa term and an effective Coulomb interaction among protons *i.e.*

$$V^{tot} = V^{Sk} + V^{Yuk} + V^{Coul}, \tag{2}$$

with local Skyrme interaction consisting of two- and three-body interactions:

$$V^{Sk} = t_1\delta(\mathbf{r}_i - \mathbf{r}_j) + t_2\delta(\mathbf{r}_i - \mathbf{r}_j)\delta(\mathbf{r}_i - \mathbf{r}_k). \tag{3}$$

Since QMD model is a n-body theory, therefore, Eq. (3) can be reduced to a density dependent potential in the limit of infinite nuclear matter limit as:

$$U^{Sk} = \alpha(\frac{\rho}{\rho_o}) + \beta\left(\frac{\rho}{\rho_o}\right)^2. \tag{4}$$

The momentum dependence of nuclear mean field is included in Eq. (2) via momentum dependent interaction as:

$$V^{MDI} = t_4 ln^2\left[t_5\left(\mathbf{p}_i - \mathbf{p}_j\right)^2 + 1\right]\delta\left(\mathbf{r}_i - \mathbf{r}_j\right), \tag{5}$$

with parameters $t_4 = 1.57\ MeV$ and $t_5 = 5.0 \times 10^{-4}\ (MeV/c)^{-2}$. This parameterization is deduced from the real part of the proton-nucleus optical potential which reproduces the experimental data upto 1 GeV/nucleon [4, 24]. In an infinite nuclear matter limit, generalized n-n potential (Eq.(2) and (5)) leads to following density and momentum dependent potential (without Coulomb and Yukawa terms):

$$U(\rho, \mathbf{p}) = \alpha \left(\frac{\rho}{\rho_0}\right) + \beta \left(\frac{\rho}{\rho_0}\right)^{\gamma} + t_4 ln^2[t_5(\mathbf{p}^2 + 1)] \left(\frac{\rho}{\rho_o}\right). \tag{6}$$

The parameters α, β and γ in Eq.(6) have to be re-adjusted in the presence of momentum dependent interactions so as to reproduce the ground state properties of nuclear matter. The parameters corresponding to soft, hard and their momentum dependent versions are labelled as S, H, SM and HM, respectively. The constants α and β give the proper rms radii and binding energies of nuclei across the periodic table. Parameter γ gives us possibility to examine the compressibility and hence equation of state. The set of parameters corresponding to soft (S), hard (H) and their momentum dependent versions SM and HM, respectively, can be found in Ref. [5].

3 Results and discussion

3.1 Stability of cold QMD nuclei

To address the question of stability of computational nucleus in the presence of momentum dependent interactions (MDI), we initialize a single cold projectile using soft (S) equation of state and soft momentum dependent equation of state (SM). Earlier theoretical attempts ranging from giant monopole resonances [25] to nucleosynthesis of heavy elements in mergers of neutron stars [26] could be explained if the equation of state (EoS) is relatively *soft* than when it is *stiff*. Another study concerning the linear momentum transfer occuring in central HI collisions also showed that a soft compressibility modulus is needed to explain the experimental data [27, 28]. These observations motivated us for the choice of comparatively softer EoS. We follow the cluster emission pattern and rms radii of few computational nuclei. Figure 1 shows the time evolution of cold QMD nuclei, namely ^{58}Ni and ^{197}Au initialized with S and SM interactions. The cluster emission is followed for the time span of 200 fm/c. Here,

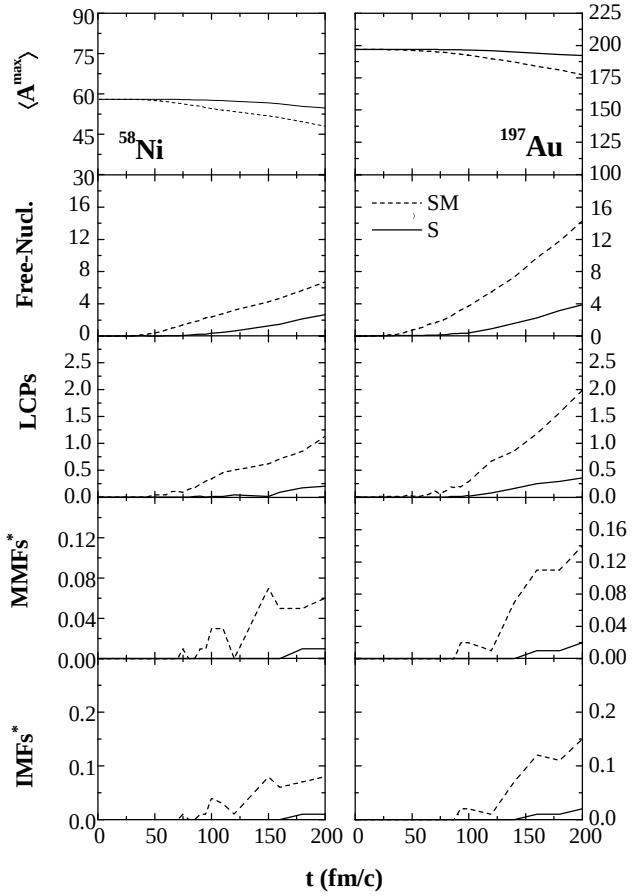

Figure 1: The time evolution of heaviest fragment $\langle A^{max} \rangle$, free nucleons, LCPs $[2 \leq A \leq 4]$, $MMFs^*$ $[5 \leq A \leq 9]$ and $IMFs^*$ $[5 \leq A \leq A_P/3]$ (A_P being the mass of projectile nucleus) emitted from a single cold nucleus of ^{58}Ni (left panel) and ^{197}Au (right panel). Results obtained with soft (S) equation of state are represented by solid lines whereas dashed lines show results with soft momentum dependent (SM) equation of state. '*' indicates that heaviest fragment has been excluded.

A^{max} denotes the size of residual nucleus. This should be close to that of parent nucleus if there is no destabilization of the nucleus. The sizes of parent

^{58}Ni and ^{197}Au nuclei reduce with the inclusion of momentum dependent interactions compared to nuclei propagating with static soft interactions alone. The SM interactions caused an enhanced emission of free nucleons and light charged particles LCPs [$2 \leq A \leq 4$]. However, medium mass fragments MMFs [$5 \leq A \leq 9$] and IMFs {[$5 \leq A \leq A_P/3$]; A_P being the mass of projectile} are almost insensitive towards momentum dependent interactions. Superscript (*) indicates that heaviest fragment has been excluded from the multiplicities of MMFs and IMFs. Only a small fraction is emitted as intermediate mass fragments (IMFs). It seems that nucleons close in space are emitted in bulk, therefore, leading to an enhanced emission of light clusters. On the contrary, very few nucleons, LCPs and heavier clusters are emitted when propagating with soft EoS. The enhanced evaporation with MDI is also due to repulsive nature of these interactions. Does this enhanced emission prohibit one to use MDI for fragmentation ? If one sees carefully, majority of mass that leaves the gold nucleus (for example, with MDI about 19 units are emitted and $\langle A^{max} \rangle$ is close to 177) is in the form of free nucleons. In the above gold nucleus, out of 19 units about 15 are in terms of free nucleons. In other words, we see that nucleons from the surface are emitted and there is no contribution towards the emission of intermediate mass fragments. One sees that even with MDI, only 0.15 IMFs are emitted on the average. Realizing that as many as 10-12 IMFs can be seen emitted in Au+Au reaction [32], this number with MDI is negligible.

A survey of the time evolution of rms radii of a single QMD nucleus also depicts the same picture. We show in Fig. 2, the time evolution of rms radii of ^{58}Ni and ^{197}Au nuclei till 200 fm/c. The rms radius of nucleus with SM interactions increases gradually compared to that initialized with static soft interactions. This behavior reflects that MDI create additional repulsions among nucleons which leads to enhanced emission of free nucleons. The rms radii of gold and nickel nuclei in soft case shows negligible deviation for the characteristic time of HI collision. As discussed above, this enhanced radius is due to the emission of free nucleons and not due to the IMFs. Therefore, one can study the fragmentation with MDI since the structure of IMFs is not altered by the inclusion of MDI.

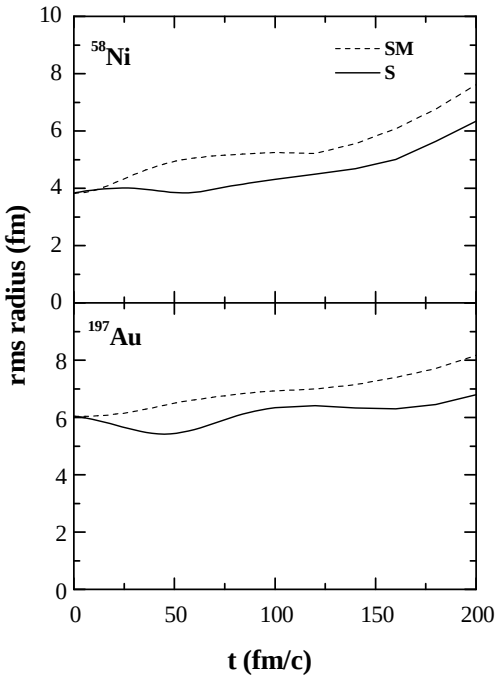

Figure 2: The time variation of rms radii of single cold nuclei of ^{58}Ni (top panel) and ^{197}Au (bottom panel) using soft (S) equation of state (solid lines) and soft momentum dependent (SM) interactions (dashed lines).

3.2 Heavy-ion collisions and system size effects

After investigating the behavior of cold nuclei initialized with momentum dependent interactions, let us study the effect of momentum dependent forces in heavy-ion reactions. One of the observables linked with the compression and expansion of nuclear matter is the density of fragmenting system. The total nuclear matter density is obtained as :

$$\rho(\mathbf{r},\mathbf{t}) = \sum_{\mathbf{j=1}}^{\mathbf{A_T+A_P}} \frac{\mathbf{1}}{(\mathbf{2\pi L})^{\mathbf{3/2}}} \mathbf{e}^{-(\mathbf{r}-\mathbf{r_j(t)})^{\mathbf{2}}/\mathbf{2L}}. \tag{7}$$

Here A_T and A_P stand for the target and projectile masses, respectively. In our approach, average nuclear matter density $\langle\rho/\rho_o\rangle$ is calculated in a sphere of 2

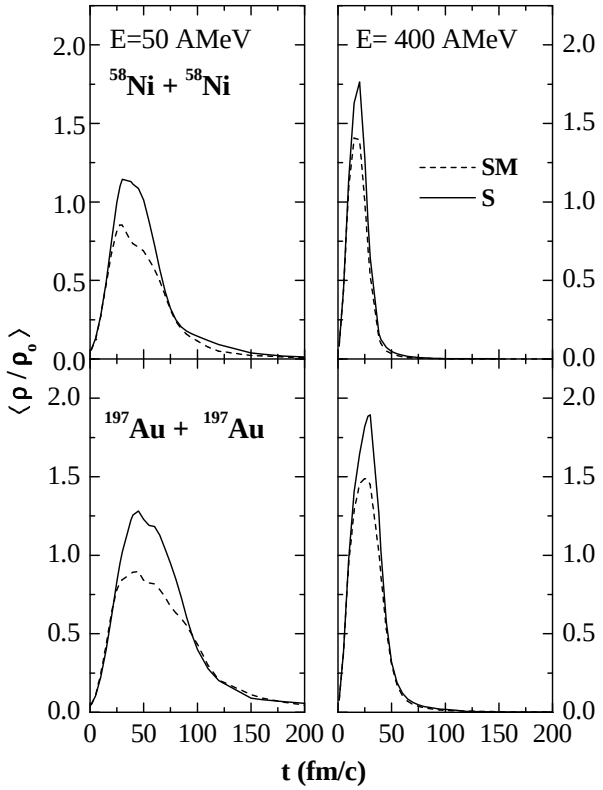

Figure 3: The average nucleonic density $\langle\rho/\rho_o\rangle$ calculated in a central sphere of 2 fm radius versus reaction time for the central collisions of $^{58}Ni +^{58} Ni$ (top panel) and $^{197}Au +^{197} Au$ (bottom panel). The results obtained with soft (S) and soft momentum dependent (SM) interactions are compared at 50 AMeV (left) and 400 AMeV (right).

fm radius.

In Fig. 3, we display the time evolution of average nucleon density $\langle\rho/\rho_o\rangle$ reached in the central region for the head-on collisions of $^{58}Ni +^{58} Ni$ and $^{197}Au +^{197} Au$ at incident energies of 50 and 400 AMeV. The maximal average density tends to reduce with inclusion of momentum dependent interactions. This happens due to additional n-n repulsions created in the system that prohibits compression of nuclear matter to a significant level. This difference in the behavior of $\langle\rho/\rho_o\rangle$ calculated using S and SM interactions diminishes at higher

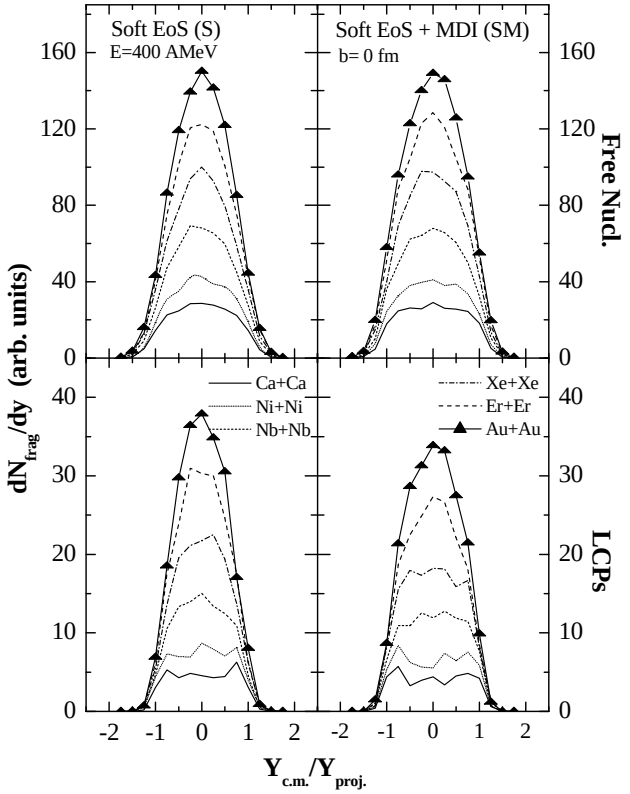

Figure 4: The rapidity distribution dN_{frag}/dy of free nucleons and LCPs [$2 \leq A \leq 4$] as a function of scaled rapidity $Y_{c.m.}/Y_{proj.}$; $Y_{proj.}$ being the rapidity of projectile for the head-on collisions at 400 AMeV.

incident energies (400 AMeV). This is due to the fact that in central collisions at 400 AMeV, most of the initial n-n correlations are already destroyed and matter is already scattered, and therefore, repulsion generated due to MDI does not play any significant role. As a result, we do not see much difference in average central density reached at higher incident energy. Another important quantity related with the initial compression of nuclear matter is the rate of binary collisions. We have also checked the collision rate for these reactions and its behavior is found to be consistent with the density profile. The rapidity distribution of nucleons is another useful tool to characterize the stopping and thermalization of the nuclear matter. We have displayed in Fig. 4, the fragment

rapidity distribution dN_{frag}/dy of free nucleons and LCPs for central collisions of six different symmetric systems at 400 AMeV. The results are displayed here using soft EoS (left panel) and soft EoS including MDI (right panel). The rapidity distribution is more 'isotropic' and nearly full stopping is achieved in heavier systems like Au+Au and Er+Er. In lighter systems, on other hand, a larger fraction of particles is concentrated near target and projectile rapidities resulting into broad Gaussian shape. This feature can be seen in both S and SM cases. The lighter systems, therefore, exhibit larger *transparency* effect *i.e.* less stopping. Such features are also observed in the experimental data of FOPI-group [29]. Based on the experimental observations and theoretical trends, one can say that smaller the system, lesser is the stopping. With MDI, a slight increase in transparency effect is seen due to lesser stopping of particles in longitudinal direction. This happens due to reduction in *n*-*n* collisions which deflect the fragments in transverse direction. As a results, one obtains less particles being stopped in longitudinal direction. The system size effects in the production probability of different kinds of fragments has been studied and predicted by our group [8]. Here we extend the same study with reference to momentum dependent interactions. For this analysis, we simulated the central collisions of six symmetric systems $^{40}Ca +^{40} Ca$, $^{58}Ni +^{58} Ni$, $^{93}Nb +^{93} Nb$, $^{131}Xe +^{131} Xe$, $^{168}Er +^{168} Er$ and $^{197}Au +^{197} Au$ at incident energies of 50 and 400 AMeV. We also parameterized the multiplicities as a function of total mass of the composite system using a power law of the form: cA_{tot}^{τ}; A_{tot} being the total mass of the system. Figure 5 displays the 'reduced multiplicity' i.e. multiplicity per nucleon of various kinds of fragments. It is clear that the system size effects are more visible in soft equation of state compared to soft momentum dependent case. A negative slope obtained for the multiplicity of free nucleons, fragments of mass A=2, and LCPs at 50 AMeV indicates their origin from the surface of interacting nuclei. As we move to momentum dependent version, additional break up of *n*-*n* correlations leads to enhanced emission of free nucleons and light charged particles. As a result, multiplicity of $MMFs^*$ $[5 \leq A \leq 9]$ and $IMFs^*$ $[5 \leq A \leq min\{A_P/3, 65\}]$ (excluding largest fragment A^{max}) gets reduced at 400 AMeV, indicating the vanishing of system size effect with MDI. In higher energy regime, cluster production via emission of $MMFs^*$ and $IMFs^*$ is strongly suppressed in the presence of MDI. It is worth mentioning that earlier studies *e.g.* see Ref. [30], also reported the momentum

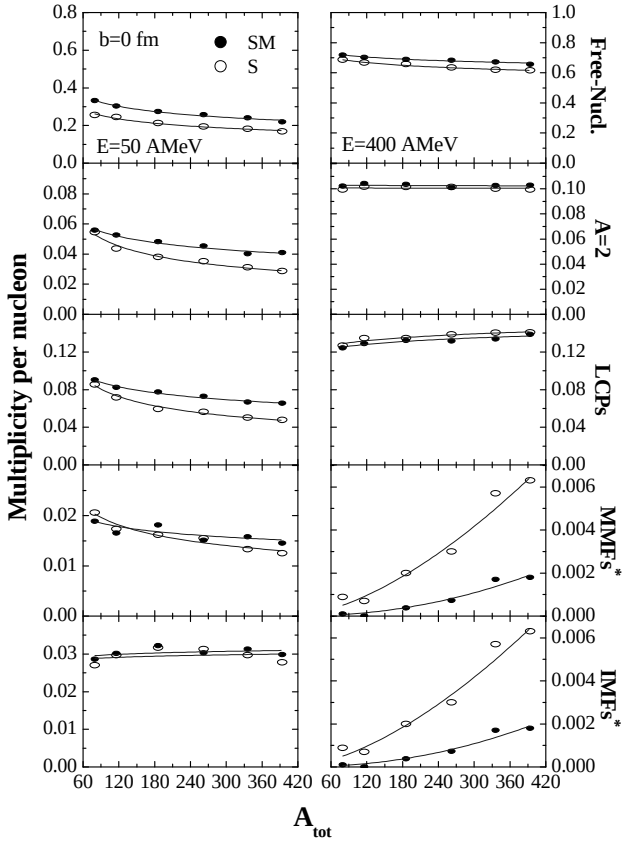

Figure 5: The final state scaled multiplicity (calculated at 200 fm/c) of free nucleons, fragments with mass A=2, LCPs [$2 \leq A \leq 4$], $MMFs^*$ [$5 \leq A \leq 9$] and $IMFs^*$ [$5 \leq A \leq min\{A_P/3, 65\}$] as a function of total mass of the system A_{tot}. Results shown here are at incident energies of 50 AMeV (l.h.s) and 400 AMeV (r.h.s). Open circles depict the calculations with soft (S) interaction while solid circles are for soft momentum dependent (SM) interactions. '*' means that heaviest fragment has been excluded.

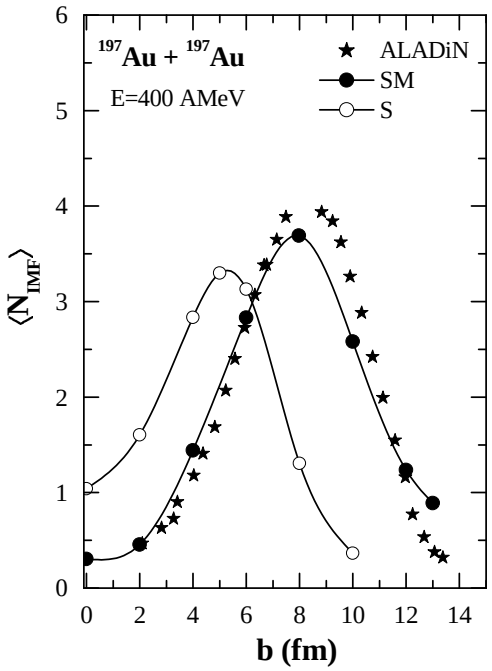

Figure 6: The mean IMF multiplicity $\langle N_{IMF} \rangle$ vs the impact parameter b for the reaction of $^{197}Au + ^{197}Au$ at 400 AMeV. The QMD calculations (at 300 fm/c) using soft EoS (open circles) and soft momentum dependent EoS (solid circles) are compared with ALADiN experimental data (filled stars).

dependent potential to be more repulsive for high momentum nucleons. This leads to enhanced emission of free nucleons and LCPs. A similar enhancement of the nucleons emission and light cluster production was predicted on inclusion of momentum dependent effective interactions in the isoscalar nuclear potential and symmetry potential [30, 31]. Contrary to this, with static soft equation of state, the production probability of MMFs and IMFs scale with the system size as power law: cA_{tot}^{τ} with power factor τ close to 3/2. Let us now try to confront our calculations with experimental data of ALADiN group [11]. The experimental data is very fascinating because it has been shown that there is a *rise and fall* of multiplicity of intermediate mass fragments with impact parameter

[11]. However universality is observed with mass of the system and with incident energies exceeding 400 AMeV. In Fig. 6, we display the multiplicity of intermediate mass fragments as a function of impact parameter using soft (S) and soft momentum dependent (SM) equations of state. We see that entire spectrum is very well reproduced by the momentum dependent interactions. One should also keep in the mind that for central impact parameters, different experimental groups like FOPI [9], ALADiN [10, 11] and Miniball [32] differ significantly in the multiplicities of IMFs. Overall, we see a clear need of momentum dependent interactions in heavy-ion collisions.

4 Summary

Summarizing these findings, we here presented a detailed study on the consequences of employing momentum dependent potential in multifragment-emission. Investigation of a single cold nucleus initialized with soft (S) and soft momentum dependent (SM) equations of state reveals that momentum dependent interactions act as *destabilizing* factor, which results into enhanced emission of free nucleons only. However, no change is seen towards artificial emission of IMFs. Further, momentum dependent interactions are observed to weaken the system size effects studied at 50 and 400 AMeV. A comparison of model calculations with ALADiN data on Au+Au reactions favor strongly the use of momentum dependent equation of state in heavy-ion collisions.

This work was supported by a research grant from Department of Science and Technology, Government of India vide grant no. SR/S2/HEP-28/2006.

References

[1] A. Ono, H. Horiuchi and T. Maruyama, Phys. Rev. C **48**, 2946 (1993).

[2] K. A. Brueckner, J. R. Bucher and M. M. Kelly, Phys. Rev. **173**, 944 (1968).

[3] N. Wang, Z. Li and X. Wu, Phys. Rev. C **65**, 064608 (2002).

[4] J. Aichelin and H. Stöcker, Phys. Lett. B **176**, 74 (1986); A. Rosenhauer, J. Aichelin, H. Stöcker and W. Greiner, J. Phys. (Paris), Colloq. **47**, C4-395 (1986).

[5] J. Aichelin, Phys. Rep. **202,** 233 (1991).

[6] G. Peilert, H. Stöcker and W. Greiner, A. Rosenhauer, A. Bohnet and J. Aichelin, Phys. Rev. C **39**, 1402 (1989).

[7] G Peilert, H. Stöcker and W. Greiner, Rep. Prog. Phys. **57**, 533 (1994).

[8] J. Singh and R. K. Puri, Phys. Lett. B **519**, 46 (2001); J. Singh and R. K. Puri, Phys. Rev. C **65**, 024602 (2002).

[9] W. Reisdorf *et al.*, Nucl. Phys. A **612**, 493 (1997).

[10] M. Begemann-Blaich *et al.*, Phys. Rev. C **48**, 610 (1993).

[11] A. Schüttauf *et al.*, Nucl. Phys. A **607**, 457 (1996).

[12] J. Pochodzalla *et al.*, Phys. Rev. Lett. **75**, 1040 (1995).

[13] J. J. Molitoris, A. Bonasera, B. L. Winer and H. Stoecker, Phys. Rev. C **37**, 1020 (1988).

[14] D. J. Magestro, W. Bauer and G. D. Westfall, Phys. Rev. C **62**, 041603(R) (2000).

[15] A. D. Sood and R. K. Puri, Phys. Rev. C **69**, 054612 (2004); Eur. Phys. J A **50**, 571 (2006).

[16] S. Soff, S. A. Bass, C. Hartnack, H. Stöcker and W. Greiner, Phys. Rev. C **51**, 3320 (1995).

[17] A. D. Sood and R. K. Puri, Phys. Rev. C **73**, 067602 (2006); R. Chugh and R. K. Puri, Phys. Rev. C (submitted).

[18] J. Aichelin, A. Rosenhauer, G. Peilert, H. Stoecker and W. Greiner, Phys. Rev. Lett. **58**, 1926 (1987).

[19] C. Hartnack, R. K. Puri, J. Aichelin, J. Konopka, S. A. Bass, H. Stöcker and W. Greiner, Eur. Phys. J A **1**, 151 (1998).

[20] D. T. Khoa, N. Ohtsuka, M. A. Matin, A. Faessler, S. W. Huang, E. Lehmann and R. K. Puri, Nucl. Phys. A **548**, 102 (1992); J. Jaenicke, J. Aichelin, N. Ohtsuka, R. Linden, and A. Faessler, Nucl. Phys. A **536**, 201 (1992).

[21] M. Berenguer, C. Hartnack, G. Peilert, H. Stöcker, W. Greiner, J. Aichelin and A. Rosenhauer, J. Phys. G: Nucl. Part. Phys. **18**, 655 (1992).

[22] S. Kumar and R. K. Puri, Phys. Rev. C **60**, 054607 (1999); Sanjeev Kumar, S. Kumar and R. K. Puri, Phys. Rev. C **78**, 064602 (2008).

[23] Jian-Ye Liu, Wen-Jin Guo, Yong Zhong Xing, Wei Zuo and Xi-Guo Lee, Phys. Rev. C **67**, 024608 (2003).

[24] S. Hama, B. C. Clark, E. D. Cooper, H. S. Sherif and R. L. Mercer, Phys. Rev. C **41**, 2737 (1990).

[25] M. Itoh *et al.*, Nucl. Phys. A **687**, 52c (2001).

[26] S. Rosswog *et al.*, Astronomy and Astrophysics **341**, 499 (1999).

[27] J. Cibor, J. Lukasik and Z. Majka, Z. Phys. A **348**, 233 (1994).

[28] F. Haddad *et al.*, Phys. Rev. C **53,** 1437 (1996).

[29] G. S. Wang, in *Proceedings of International Research Workshop, Poiana Brasov, Romania, October, 1996*, edited by M. Petrovici, A. Sandulescu, D. Pelte, H. Stöcker and J. Randrup, (World Scientific, Singapore, 1997), p. 182.

[30] Lie-Wen Chen, Che Ming Ko and Bao-An Li, Phys. Rev. C **69**, 054606 (2004).

[31] V. Greco, A. Guarnera, M. Colonna and M. Di Toro, Phys. Rev. C **59**, 810 (1999).

[32] M. B. Tsang *et al.*, Phys. Rev. Lett. **71**, 1502 (1993); G. F. Peaslee *et al.*, Phys. Rev. C **49**, R2271 (1994).